Dual channel formation in a laser-triggered spark gap

M. J. Kushner, W. D. Kimura, D. H. Ford, and S. R. Byron
Spectra Technology, Inc. (formerly Mathematical Sciences Northwest, Inc.), 2755 Northup Way, Bellevue, Washington 98004

(Received 19 June 1985; accepted for publication 12 August 1985)

During self-break in spark-gap switches, multiple streamers can form in close proximity to one another. The rate of expansion of these streamers is sufficiently fast that they can interact during the current pulse. To help understand how these closely spaced, expanding spark columns interact, a laser-triggered spark gap has been studied in which two parallel columns (separation 1.3 mm) are simultaneously preionized, resulting in a pair of nearly identical, axisymmetric spark columns. The spark gap (electrode separation 1.2 cm) switches a 100 ns, 40–60 kV, 12-20 kA, 1.5 Ω waterline. Interferograms of the expanding arc channels are obtained with a laser interferometer having a time and spatial resolution of 5 ns and 10 μm, respectively. Voltage and current were measured with an internal capacitive-voltage divider and a current viewing resistor. The interferograms show that for initially identical axisymmetric columns, the individual channels do not merge into a single larger axisymmetric spark column. Instead, regions of high gas density remain inside the combined column long into the recovery period. The columns also do not remain axisymmetric as they grow, indicating a long-range interaction between the channels. The voltage drop and resistance of the dual channel spark gaps changes by less than 15% from that of a single spark channel. A scaling model is presented to explain the resistance measurements and to predict the change in resistance for multichannel spark gaps.

I. INTRODUCTION

During self-break of spark gaps, many breakdown filaments may be formed, resulting in the spark gap operating through many individual channels. The rate of expansion of the breakdown filaments may be sufficiently rapid, and the spacing of the breakdown filaments may be sufficiently small, that during the current pulse, the arc channels interact with one another. In many instances, it is desirable to have the spark gap operate through many channels. Multichannel operation of spark gaps and rail gaps has long been recognized as a technique whereby the resistive loss and circuit inductance of the device can be reduced[1,2]; however, the optimum spacing of the arcs in rail gaps tends to be large (many millimeters to a centimeter) as compared to the spark-channel diameter (approximately 1 mm) suggesting that the arc channels can be too closely spaced.[1] The characterization of closely spaced, expanding arc channels is therefore of interest for understanding the operation of both self-breaking spark gaps and multichannel rail gaps.

The development of laser-triggered spark gaps has provided the means whereby large electrical powers (megavolts at mega-amps) can be switched at voltages significantly less than the self-break value and with jitter less than a few nanoseconds.[3–8] The use of laser preionization triggering also produces a readily reproducible plasma channel between the spark-gap electrodes that is amenable to study by laser interferometric techniques. In this paper we report on studies of a laser-triggered spark gap where two closely spaced parallel spark channels are preionized simultaneously. This preionization scheme results in a pair of nearly identical, reproducible expanding arc channels which can be studied both interferometrically and electrically. The spacing of the spark columns, 1.3 mm, is sufficiently small that they interact during a portion of the 100-ns current pulse. The diameter of each spark channel is obtained from the interferograms with a spatial resolution of better than 10 μm and a time resolution of better than 5 ns. A capacitive-voltage divider was designed specifically for use in this particular spark gap in order to give an unambiguous measure of the voltage drop between the spark-gap electrodes. This voltage measurement can then be used to calculate the resistance of the spark channels.

The results of our study of dual laser triggering in SF_6, Xe/H_2, and $SF_6/N_2/He$ gas mixtures show that the individual arc channels do not coalesce into a single-arc channel but retain their individual character long into the recovery period. Gas mixtures containing heavy molecules such as SF_6 retain this individuality to a greater extent than gas mixtures containing light gases, such as H_2. In light gas mixtures turbulent mixing may occur at the interface of the two channels. The spark channels differ from the shape of a single channel before the dual channels actually touch, thereby indicating the presence of a long-range interaction. Measurements of the resistance of dual spark channels show only a small (less than 15%) reduction as compared to the resistance of a spark gap operating through a single channel for otherwise identical conditions.

The experimental apparatus, diagnostics, and data reduction techniques are described in Sec. II. The interferometric study of dual arc formation in a laser-triggered spark gap is summarized in Sec. III. Experimental determination of the resistance of the arcs appears in Sec. IV where we also present a scaling model for the resistance of spark gaps operating through multiple arcs. Concluding remarks are in Sec. V.

II. EXPERIMENTAL APPARATUS

The experimental system, described in detail elsewhere,[9] is shown in Fig. 1. The apparatus consists of a 1.5-Ω, 100-ns waterline which is pulse charged in 1.8 μs by a two-

 0021-8979/85/234015-09$02.40

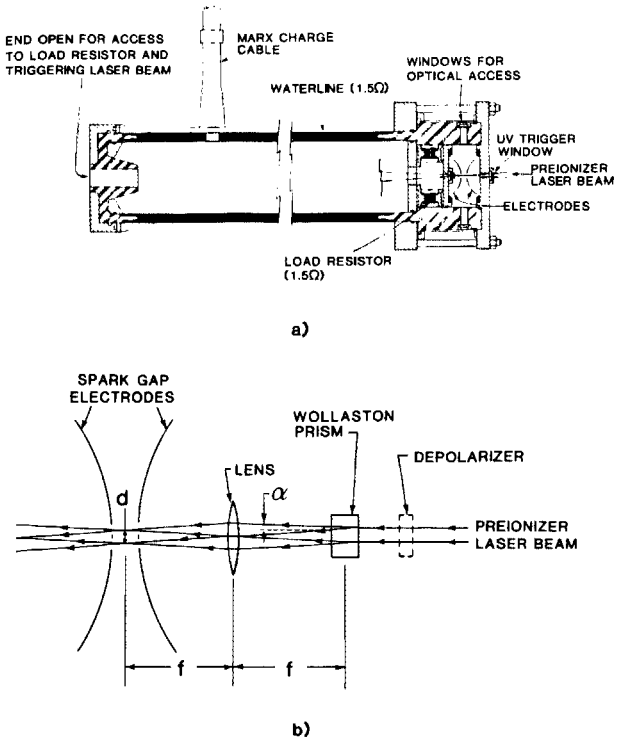

FIG. 1. Schematic of experimental apparatus. The 1.5-Ω, 100-ns water pulse forming line is terminated by a liquid copper sulfate load resistor, and switched by the laser preionization triggered spark gap. The preionization laser passes through a Wollaston prism in which perpendicular polarizations are dispersed by an angle α. A lens focuses the two individual beams, entering and leaving the interelectrode gap coaxially through a pair of 1-mm holes in each electrode, separated by 1.3 mm. The minimum electrode spacing is 1.2 cm. The spark-gap chamber is located in one leg of a Mach–Zender interferometer. The probe beam for the interferometer interrogates the arc perpendicular to the axis of symmetry. The probe laser enters and leaves the spark-gap chamber through the optical access windows indicated.

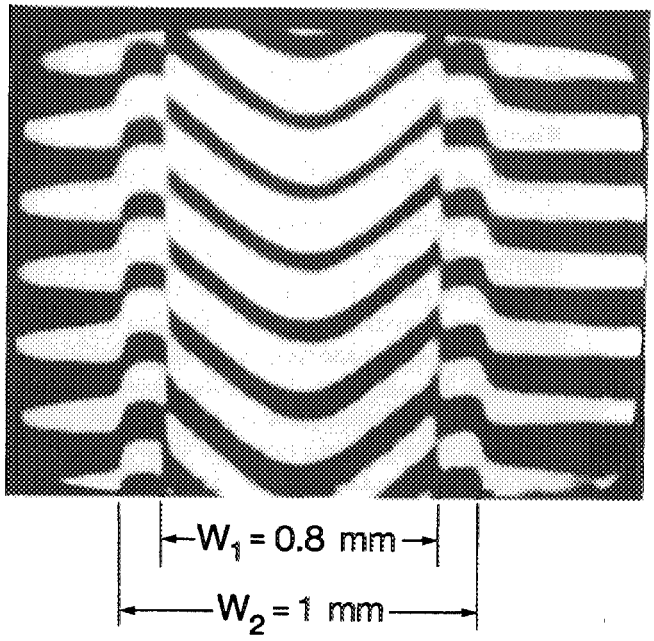

FIG. 2. Typical interferogram of the arc in a laser preionization triggered spark gap taken 40 ns after breakdown. The gas mixture is 2 atm of Xe/H_2:0.01/0.99. The voltage on the waterline at the time of triggering is approximately 40 kV. The time resolution of the interferogram is < 5 ns. The diameter of the laser preionized region at $t = 0$ is $\simeq 50\ \mu$m. The width w_1 indicates the diameter of the current carrying core of the arc. The width w_2 indicates the total diameter of the arc, including a high density, largely neutral shell surrounding the ionized core.

stage Marx bank to a voltage of 40–60 kV. Attached to the waterline is a chamber which houses a laser-triggered spark gap.

All the work described in Ref. 9 deals with single-channel laser-triggered arcs. To produce two arcs simultaneously and in close proximity to each other, the optical delivery system for the preionization laser beam described in Ref. 9 was modified as follows.

For the dual channel experiments, the spark gap consists of two hemispherical copper electrodes placed 1.2 cm apart, each having a pair of 1-mm-diam holes separated by 1.3 mm at their centers. The preionization laser beam is split into two separate beams by a Wollaston prism. The deflection angle α is $\simeq 0.4°$ and the focal length of the focusing lens is 18 cm. To ensure equal laser energy in the two beams, a depolarizer is used before the Wollaston prism. The two beams enter the electrode gap through the pair of holes in the anode, are focused at a point midway between the electrodes, and pass through the opposite holes in the cathode without striking either of the electrodes.

The spark-gap chamber is located within one leg of a laser interferometer which is used to measure details of the spark channel internal structure with a spatial resolution of better than 10 μm. The laser interferometer, also described in Ref. 9, provides a measure of the diameter of the current carrying portion of the spark column with a time resolution of < 5 ns. This diameter is used to calculate the inductance of the spark column in the manner described below.

A typical interferogram of a laser-triggered single-arc channel obtained with the laser interferometer is shown in Fig. 2. The outermost fringe shift is due to shockwave compression of the ambient gas. The downward fringe shift and the abrupt fringe jump are caused by a rapid rise in the ionization of the gas resulting in a core of high-electron density. Reference 9 provides a detailed description of the interferometer measurements of a single-arc channel.

In order to calculate the resistance of the arc in a spark column, the voltage drop across and current through the arc channel must be determined accurately. The current through the spark column is measured with a current viewing resistor (CVR). The CVR consists of an Inconel foil surrounding the spark-gap chamber. The CVR completes the current return path between the switch and load resistor, and the waterline. The voltage drop between the spark-gap electrodes is measured with a capacitive-voltage divider (CVD) specifically designed for use in this spark-gap chamber. The CVD and the processing of its signal are discussed in detail in Refs. 10–12. The CVD is mounted within the spark-gap chamber in a manner to minimize the inductance of the CVD and to minimize the inductive component of the voltage measured by the CVD. The rise time of the probe is estimated to be less than 1 ns. Typical current and voltage waveforms obtained with our probes are shown in Fig. 3.

The time dependent resistance of the arc in the spark gap $R_s(t)$ is simply $V_r(t)/I(t)$, where $V_r(t)$ is the resistive vol-

tage drop across the arc and $I(t)$ is the total current. However, the voltage measured by the CVD is

$$V_0(t) = I(t)R_s(t) + [L_s(t) + L_f]\frac{dI(t)}{dt} + I(t)\frac{dL_s(t)}{dt}, \quad (1)$$

where $L_s(t)$ is the time varying inductance of the spark column and L_f is a constant inductance value attributable to the geometry of the electrodes (≈ 5 nH). For our conditions, the last term in Eq. (1) is small and can be neglected. To obtain $R_s(t)$ from Eq. (1), the measured voltage and current waveforms (as they appear in Fig. 3) are digitized and entered as inputs to a computer program. In the program, the current waveform is numerically differentiated to provide $dI(t)/dt$. The last remaining quantity required to solve for $R_s(t)$ is the spark channel inductance $L_s(t)$. This value is obtained from the time history of the spark-channel radius as measured from laser interferograms taken coincidently with the voltage and current measurements. Assuming current flows uniformly through the spark column, the value of $L_s(t)$ is given approximately by

$$L_s(t) \cong l\frac{\mu_0}{2\pi}\ln\left(\frac{r_c}{r_s(t)}\right), \quad (2)$$

where l is the length of the spark column, r_c is the radius of the current return path (≈ 14 cm), and $r_s(t)$ is the radius of the spark channel obtained from the interferograms. For closely spaced dual channels we used the approximation that $r_{\text{dual}}(t) = 2\ r_s(t)$, where $r_s(t)$ is the radius of one of the two identical channels. The inductance of k similarly closely spaced channels is $L_k \propto \ln(1/k)$. With this value of $L_s(t)$, it is possible to solve for the spark channel resistance $R_s(t)$ from Eq. (1). For many widely spaced channels as found in rail gaps (spacing $>$ channel diameter), the inductance of k channels is $L_k \approx L_1/k \propto 1/k$ (Ref. 1). Due to the close proximity of the channels in our spark gap, the inductive contribution to the voltage fall time is only moderately reduced as compared to an otherwise identical pair of widely spaced arc channels, as found in rail-gap switches.

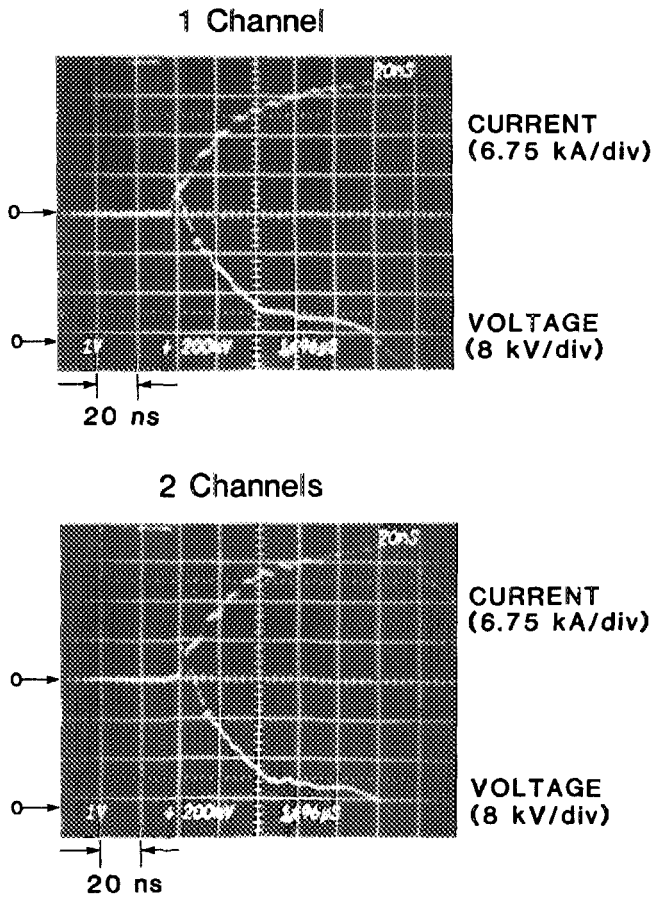

FIG. 3. Current and voltage traces for the laser-triggered spark gap shown in Fig. 1 operating through a single channel (upper figure) and two channels (lower figure). The gas is 1.0 atm SF_6 and the line voltage at triggering is 56 kV.

III. LASER INTERFEROMETRIC MEASUREMENTS OF LASER PREIONIZATION TRIGGERED DUAL SPARK COLUMNS

The successful formation of parallel, dual spark channels is a sensitive function of the relative amounts of preionizer energy in the two laser beams. If the distribution of energy is not equal, then the channel with the higher amount of preionizer energy avalanches into a fully developed spark column while the channel with the smaller amount of preionizer energy does not. This effect is discussed in more detail below. We were able to prevent this from occurring by inserting a depolarizer before the Wollaston prism to assure nearly equal laser energy in each beam.

The ability to obtain simultaneous dual channels was found to be not only a function of the relative distribution of preionizer energy between the two beams, but also of the absolute amount of laser energy and the fraction of self-break voltage applied to the gap. In general, for a given amount of evenly distributed preionizer laser energy, the probability of simultaneity increases as the charging voltage approaches the self-break value. If the charging voltage is too low, or for a given charging voltage the amount of laser energy is too small, the spark channel will randomly develop through one of the two channels, but not both. Similar behavior was observed by Taylor and Leopold[1] in a multichannel rail gap and by Hajes *et. al.*[14] in their study of widely spaced laser-triggered spark channels. The latter experiments used a geometry where the laser is focused on one of the electrodes. With sufficient laser power in each beam ($\approx 200\,\mu$J, 5 ns), reproducible, axisymmetric, and equal size dual spark channels are obtained. Temporal jitter is < 5 ns, and spatial jitter is $< 10\,\mu$m.

A typical sequence of channel formation in a laser-triggered dual spark column appears in Fig. 4. The gas mixture is $SF_6/N_2/He$:0.05/0.20/0.75, the gas pressure is 2 atm, and the charging voltage is ≈ 40 kV. The voltage corresponds to $F_{SB} = 0.7$, where F_{SB} is the fraction of the dc self-break voltage that the waterline is charged to at the time of laser triggering. The time the interferogram is taken with respect to the start of the current pulse is denoted by Δt.

The columns initially expand symmetrically about their respective vertical axes. A single channel will continue to expand in this radially symmetric fashion. With dual channels, though, as the channels expand and move closer to each

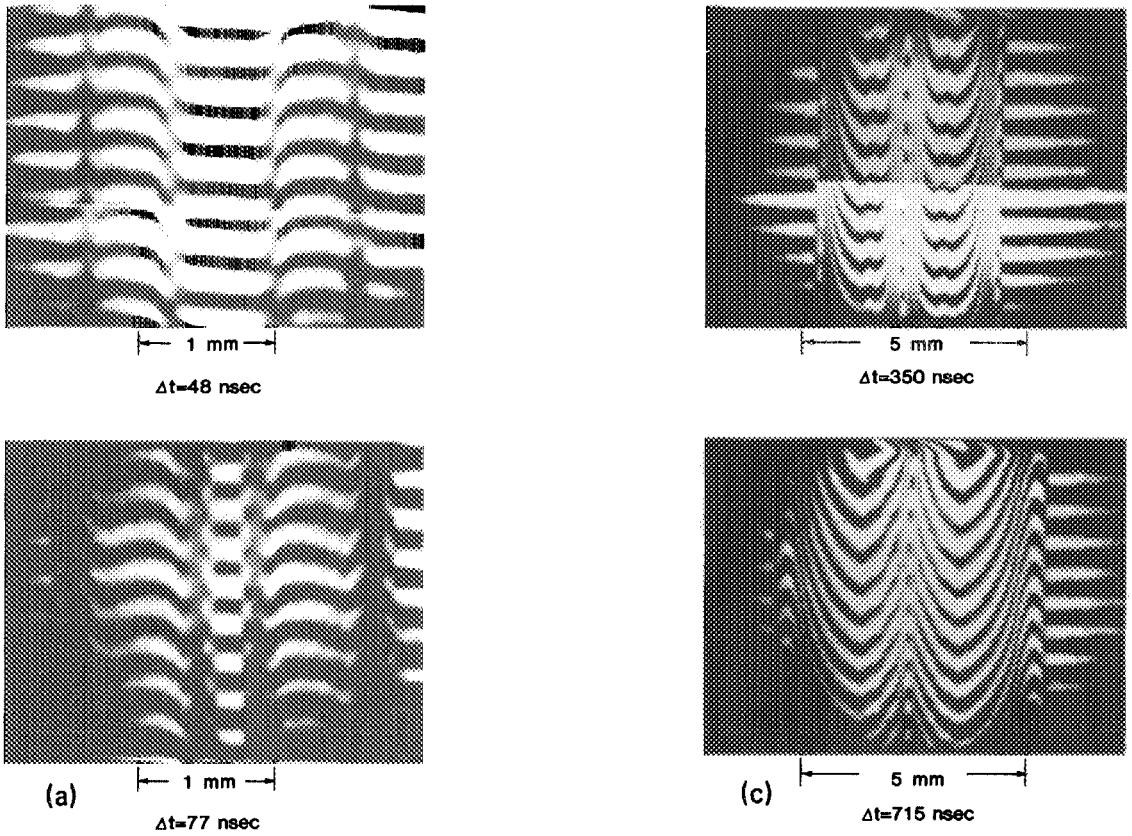

FIG. 4. Laser interferograms for the expansion of dual channels in a $SF_6/N_2/He$:0.05/0.20/0.75 gas mixture. The initial pressure is 2 atm and the line voltage at triggering is 38 kV. The indicated time is the delay after laser triggering. The duration of the current pulse is ≈ 100 ns. Note the change in spatial scale. The interferogram is centered between the spark-gap electrodes, separated by 1.2 cm.

other, they become asymmetric with respect to their individual central axes. This asymmetry occurs before the high-density shells surrounding the rarified ionized core actually touch. In the second interferogram ($\Delta t = 48$ ns) the edges of the columns are still separated by greater than 0.6 mm; however the inner edges of each column are distorted and distinctly different from the outer edges. The outer edges of the columns retain the characteristic shape seen for single spark columns. As the spark columns in Fig. 4 continue to expand, the centers of the columns also appear to approach each other. These observations may be explained by one or a combination of two effects. First, ultraviolet radiation from the opposite spark column may enhance the local rate of ionization, and hence expansion, on the near side of the adjacent column, thereby distorting the shape from that of the undisturbed edge on the opposite side. Second, the $\mathbf{u}\times\mathbf{B}$ force associated with the parallel conducting channels provides a sideways force of approximately 2×10^{-15} nt per charge carrier as compared to 8×10^{-14} nt in the vertical direction provided by the applied electric field. The fractional sideways deflection will be approximately 4% of the longitudinal drift distance.

When the spark columns finally collide, the individual character of each column is retained; that is, there does not appear to be a "coalescing" of the two spark columns into a single column. This behavior is a function of the gas mix, as will be discussed below. For these conditions, the observed individual character of the spark channels implies that during selfbreak, individual filaments will not expand and merge into a single large spark column. Obtaining interferograms with our pulsed laser interferometer of self-breaking spark gaps to confirm this hypothesis is difficult due to the large temporal and spatial jitter associated with self-breaking spark columns. However, a small selection of such interferograms have been obtained under self-breaking conditions, an example of which appears in Fig. 5. From the size of the columns, we estimate that this interferogram was obtained approximately 50 ns after self break. Note that for these multichanneling conditions, adjacent self-breaking filaments do not coalesce into a single large conducting channel. The individual character of the separate breakdown filaments is retained during the conduction phase of the current pulse in a fashion very similar to that demonstrated here with laser triggering. In self-breaking switches, though, the plasma column is very often turbulent and fails to show the symmetric well-ordered structure displayed in the interferograms of the self-breaking spark column in Fig. 5.

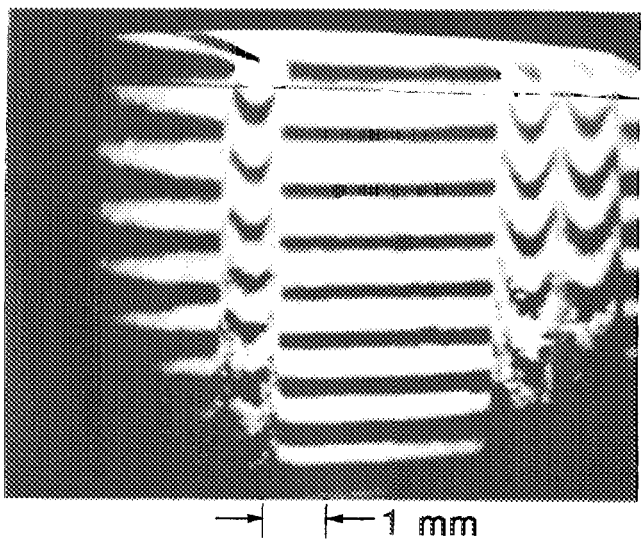

FIG. 5. Interferogram of a self-breaking spark with no laser triggering in a mixture of Xe/H_2:0.01/0.99 approximately 50 ns after breakdown. The initial gas pressure is 2.0 atm and the line voltage at triggering is $\simeq$54 kV.

A sequence of interferograms for a dual spark channel in a Xe/H_2:0.01/0.99 gas mixture is shown in Fig. 6. The dual spark columns for this lighter gas mixture have the same qualitative behavior as that of the heavier gas mix discussed above. Because the lighter gas mixture expands more rapidly, for a fixed initial separation, the columns collide at an earlier time and become nonsymmetric (with respect to their own axes) earlier than with the heavier gas mix in the previous example. In addition to the more rapid rate of expansion in the lighter gas mix, there also appears to be turbulent mixing of the two columns at their interface. The depth of the turbulent mixing region increases as the columns grow larger, although the rate of growth of the turbulent region is smaller than the sum of the rate at which the individual columns are expanding.

The last frames of Figs. 4 and 6 are at time delays longer than the current pulse (duration 100 ns). The individual character of the two columns are retained for a very long time into the recovery phase. Recovery appears to progress individually in each column rather than by a mixing of the two. When two columns are initiated with nearly identical amounts of preionization laser energy, the columns conduct the same amount of current and grow at nearly identical rates. For these conditions, when the opposing high-density shells meet each other a region of stagnation develops between them. This is not the case if the two columns do not start with equal amounts of preionization energy; one channel carries more current than the other and grows more rapidly. The shock of the larger channel is stronger than that of the smaller channel and is transmitted through the weaker shock into the interior of the smaller channel. A series of interferograms illustrating this sequence of events is shown in Fig. 7.

IV. ARC RESISTANCE OF SPARK GAPS WITH DUAL LASER-TRIGGERED CHANNELS

Current and voltage traces for dual spark columns were obtained and compared with those for single spark columns having otherwise identical conditions. A typical pair of *I-V* characteristics appear in Fig. 3. The total resistances of the dual and single spark columns were determined in the manner described in Sec. II and are plotted in Fig. 8 for SF_6 and $SF_6/N_2/He$ gas mixtures. One would expect that with the dual channel acting like two parallel resistors, the voltage drop would be significantly less than with a single channel. However, a qualitative inspection does not reveal a significant decrease in the voltage drop across the channel with dual channels as compared to a single channel. A similar observation was made by Hajes *et al.* in Ref. 14. The total

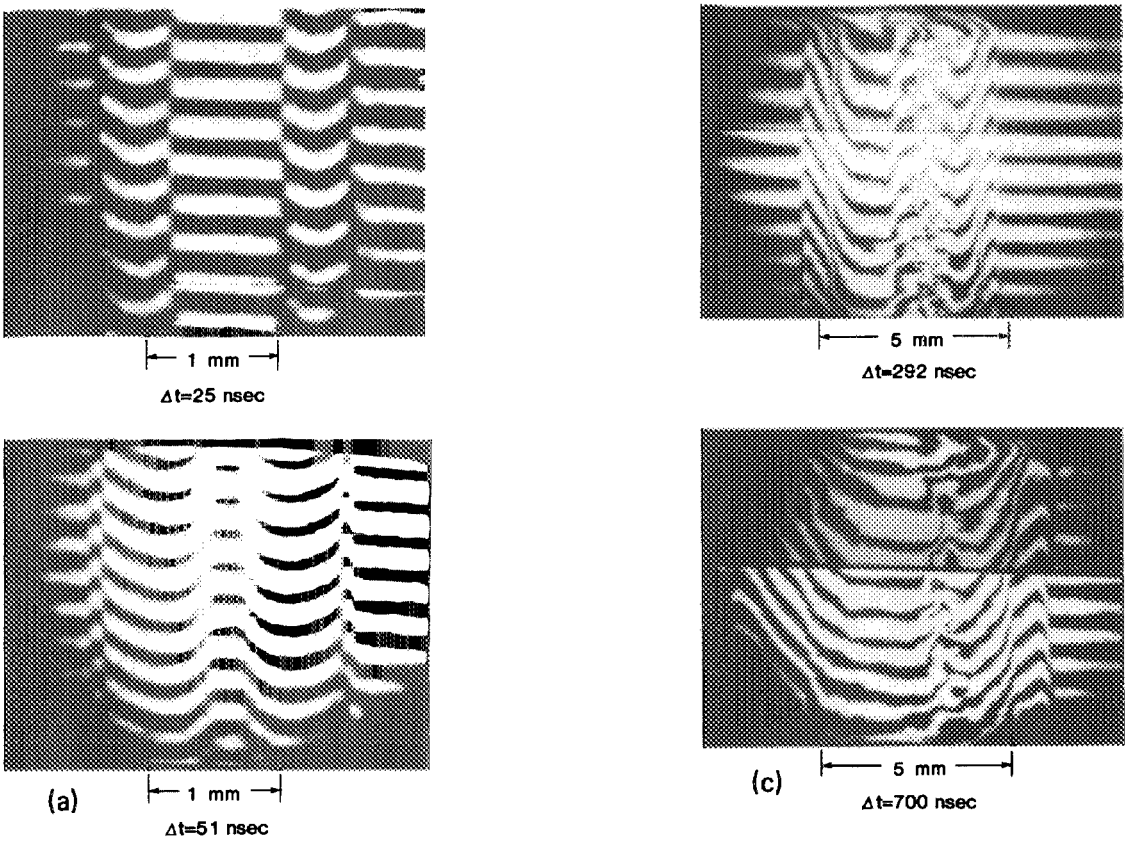

FIG. 6. Laser interferograms for the expansion of dual channels in a Xe/H_2:0.01/0.99 gas mixture. The initial pressure is 2 atm and the line voltage at triggering is 40 kV. The indicated time is the delay after laser triggering. The duration of the current pulse is $\approx$100 ns. Note the change in spatial scale.

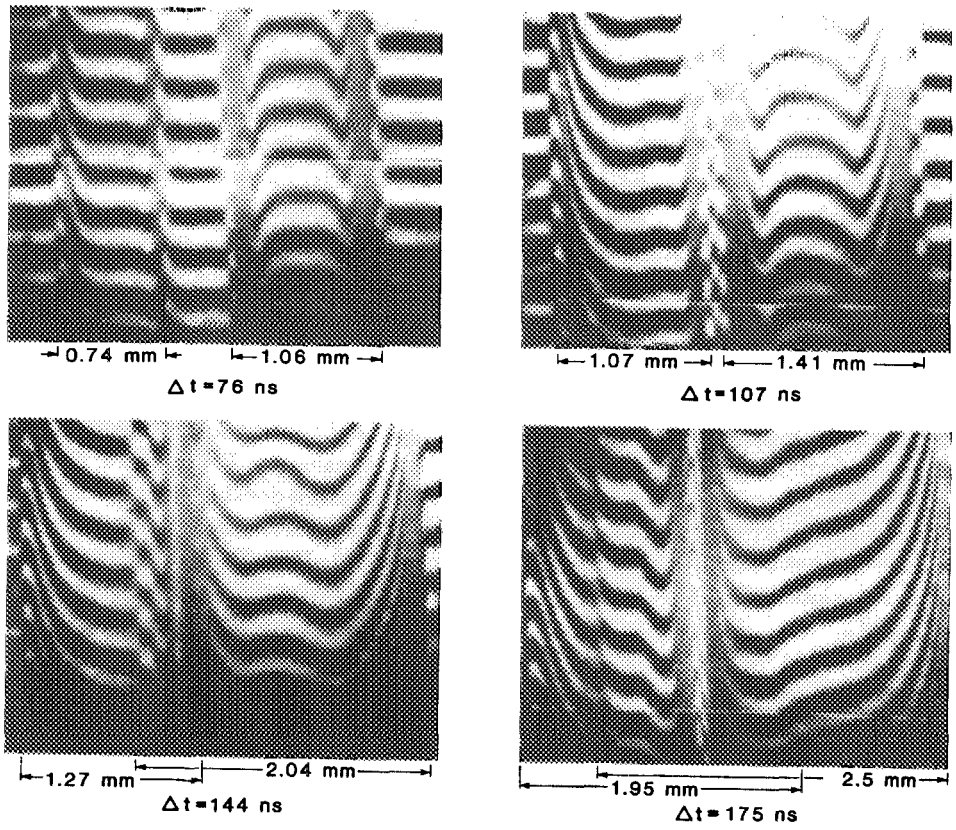

FIG. 7. Laser interferograms for the expansion of dual channels in a SF_6/N_2/He:0.05/0.20/0.75 gas mixture for unequal amounts of laser preionization energy. The initial pressure is 2 atm and the line voltage at triggering is 40 kV. The indicated time is the delay after laser triggering. The duration of the current pulse is $\simeq 100$ ns. Note the penetration of the stronger shock of the larger spark column through the weaker shock of the smaller column.

resistance of the dual spark channels is also unexpectedly large, and is only marginally (10–15%) less than that of a single spark channel.

There are two effects that account for the large voltage drop and resistance of the dual channels. First, the two spark columns are too close to each other, as compared to the dimension of the current return path, to significantly change the inductance of the gap. If the sparks were separated by a large distance, the inductance of the column could be reduced significantly. For our conditions, the inductive voltage drop therefore does not significantly change.

The second effect that accounts for the large voltage drop and resistance for the dual channels has to do with the specifics of the conductivity of the plasma columns. The degree of ionization of the arcs has exceeded the value required to reach Spitzer conductivity (1–10% ionization is sufficient). In this limit, the electrical conductivity of the plasma σ is nearly independent of the degree of ionization and is proportional to $T_e^{3/2}$, where T_e is the electron temperature.[15] The electron temperature is in turn a function of the rate of joule heating of the plasma, j^2/σ, where j is the current density. As a result of having two spark channels, the electron temperature decreases due to the sharing of current (which reduces j) between the two columns. The decrease in electron temperature reduces the conductivity of the column, and thereby increases the resistance of the spark column and (for constant current) increases the voltage drop. This sequence of events is described by the following simple model.

We assume that each of the dual spark columns is identical and that current is equally shared between them. We also assume that the arcs are in local thermodynamic equilibrium

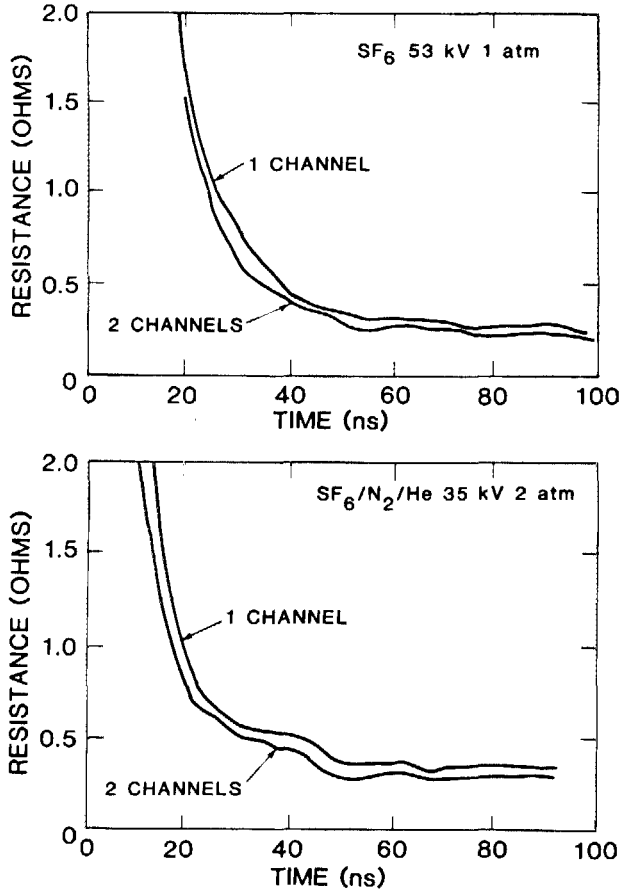

FIG. 8. The resistance of the arc in single and dual channel spark gaps for SF_6 (upper figure) and SF_6/N_2/He:0.05/0.20/0.75 (lower figure) as a function of time after triggering. These results were obtained by removing the inductive component of the measured voltage in the manner described in Sec II.

(LTE) and that the electrical conductivity is given by the Spitzer value. For LTE conditions, $T_e = T$, where T is the gas temperature. In addition we stipulate that T is proportional to the instantaneous heating rate per atom, $j(t)^2/[N(t)\sigma(t)]$, where j is the average current density, and N the atom number density. If no mass is entrained into the arcs and the arcs grow predominantly by hydrodynamic expansion of the ionized core (also known as the snow-plow model) then $N(t) \propto A_0 P_0 / A(t)$ where P_0 is the initial gas pressure, A_0 is an "initial" area of the arc, and $A(t)$ is the cross-sectional area of the arc. In a previous analysis of the arc resistance of laser triggered spark columns operating through a single channel[12] we found that $A_0 \propto F_{SB}$ yielded excellent agreement with experiment. This assignment was made, based on estimates of the initial nonconvective expansion of the arc and results from a model for laser-triggered spark gaps.[13] We extend the analysis to arcs operating through k channels and assign $A_0 \propto F_{SB}/k$. This assignment reflects the energy available per channel for nonconvective expansion of the arc to its "initial" area of A_0.

From our interferometric measurements of arc size, we found that the diameter of the arc channel increases almost linearly with time so that $A(t) = \pi(\rho t)^2/4$, where ρ is the rate of expansion of the diameter of the arc. With these assumptions, we have for the gas temperature T and the total resistance R_k of k arcs,

$$T \propto \frac{j^2}{N\sigma} \propto \left(\frac{I}{kA}\right)^2 \frac{kA}{F_{SB} T^{3/2} P_0} \rightarrow T \propto \left(\frac{I^4}{(kF_{SB} P_0 A)^2}\right)^{1/5}, \quad (3)$$

$$R_k \propto \frac{1}{k\sigma A} \propto \frac{1}{kT^{3/2}A} \propto \frac{1}{k}\left(\frac{(kF_{SB}P_0)^3}{A^2 I^6}\right)^{1/5} \propto \left(\frac{F_{SB}^3 P_0^3}{k^2 \rho^4 I^6}\right)^{1/5}. \quad (4)$$

We see that as the arc expands, the resistance of the arc decreases simply as a result of the increase in the cross-sectional area of the arc. But as the cross-sectional area increases, the temperature of the arc decreases as a result of a lower volumetric heating rate. The resistance of the arc is therefore a convolution of these two opposing effects. The average electrical conductivity of the arc may in fact decrease simultaneously to the total resistance decreasing provided that the area of the arc increases at a sufficiently high rate. The result of these opposing effects is that the resistance of an individual arc ($k = 1$) decreases proportionally to $A^{-2/5}$ instead of A^{-1}. By operating through two arcs ($k = 2$), the resistance is lowered as a result of having two resistors in parallel. Simultaneously, though, current is shared between the two channels, thereby reducing the heating rate, decreasing the electron temperature, and decreasing the conductivity of the individual arcs. Resistance is therefore increased.

Assuming the current remains equal (accurate to better than 5% for our conditions) and for equal values of F_{SB} and P_0, the ratio of arc resistance for multiple arcs as compared to single arcs is

$$\frac{R_k}{R_1} = \left(\frac{\rho_1}{\rho_k}\right)^{4/5} \frac{1}{k^{2/5}}. \quad (5)$$

The opposing effects of reducing resistance by having parallel conductors and reducing conductivity by sharing current combine with the result that the total resistance of the spark gap changes only by the 2/5 power of the number of channels instead of inversely proportional to the number of channels. For our laser-triggered dual spark channels in $SF_6/N_2/He$ mixtures as appeared in Figs. 4 and 8, we use the experimentally measured values for ρ ($\rho_1/\rho_2 = 1.3$) in Eq. (5) and find $R_2/R_1 = 0.94$. This value agrees quite well with the experimental value of 0.90, thereby giving credence to our simple model. For the pure SF_6 case (Fig. 8), our simple model yields $R_2/R_1 = 0.86$ and the experimental value is 0.89.

In order to extend our simple model to a spark gap operating through more than two channels, we must have a relationship between the rate of arc expansion ρ and the number of channels. If we assume the expansion of the channel is sonic, then the rate of expansion $\rho \propto T^{1/2}$ and $A \propto T$ so that $R_k/R_1 = k^{-2/7}$. With this relationship for two columns, $R_2/R_1 = 0.82$, which compares favorably with the experimental value for SF_6 of 0.89. This relationship implies that for the resistance of a closely spaced multichannel spark gap to be half that of a single channel spark gap, the multichannel spark gap must operate through 11 arcs.

One of the conclusions obtained with our simple model is that as a result of current sharing between a pair of spark channels, the heating rate is less than for a single channel and therefore the electron temperature and conductivity are lower than for a single channel. This conclusion is difficult to directly verify, however it can be indirectly verified from the interferograms in Fig. 9. The interferograms are for arcs in a Xe/H_2:0.01/0.99 gas mixture ($V \approx 38$ kV, $P_0 = 2$ atm) for operation through single and dual laser preionized channels. The conditions are otherwise identical. Recall that the downward shift in fringes in the middle of the column is dominantly a result of a core with a high-electron density ($n_e > 5 \times 10^{18}$ cm^{-3}).[9] In the interferogram for the single channel the fringe shift at the center of the arc (per mm of arc diameter) is 1.2/mm; for the dual channels this value is 0.9/mm. We see that the electron density for a single arc is larger than that for each of the dual arcs, and by inference, the electron temperature is also larger for the single arc than for each of the dual arcs.

Taylor and Leopold,[1] using the resistive phase expression of Martin,[16] predicted that the resistive losses of k widely spaced arc channels in a laser-triggered rail-gap switch should scale as $k^{-(1/3)}$. Their measurements of energy dissipation in a multichannel switch though, showed an increase in switch dissipation, and by inference an increase in R_k, when k was sufficiently large. They concluded that resistive losses in a multichannel rail-gap switch can increase when the current per channel falls below a critical value after which the resistivity of the individual channels increases. This conclusion is consistent with our simple model where the resistivity of an arc increases due to a decrease in the plasma temperature resulting from current sharing between multiple arcs.

V. CONCLUDING REMARKS

Laser preionization triggering was used to form a pair of parallel, symmetric, closely spaced (1.3 mm) spark channels, and these channels were investigated using a pulsed laser

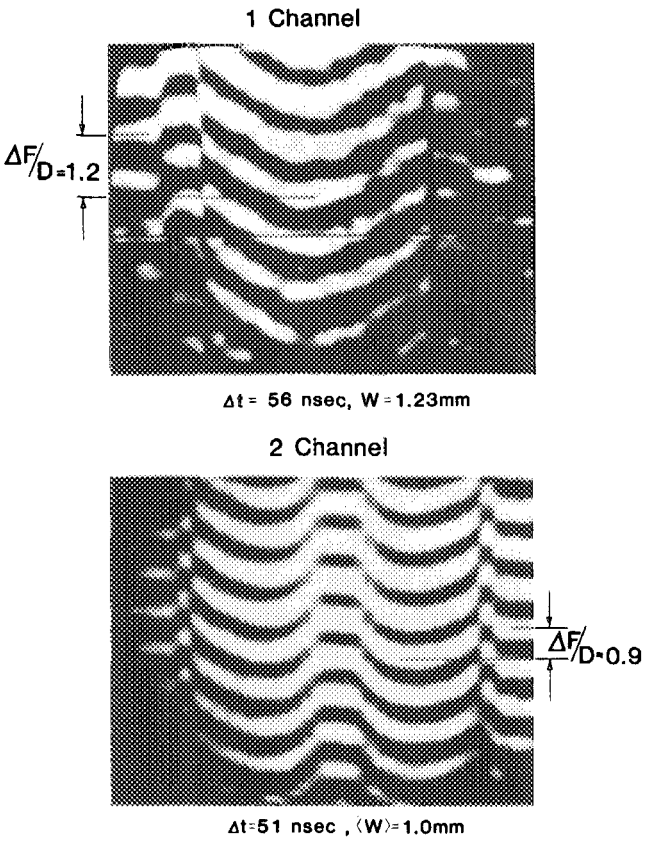

FIG. 9. Laser interferograms for single and dual channel sparks in Xe/H_2:0.01/0.99 indicating the larger fringe shift in the single channel. The notation $\Delta F/D$ is the fringe shift per mm of column width. The larger fringe shift for the single column is a result of a higher-electron density and by inference a higher-electron temperature.

laser interferometer and electrical probes. The rate of expansion of the arc channels is sufficiently fast that the channels collide during a portion of the current pulse (100 ns). The channels maintain their individual character and do not coalesce into a single channel due to the formation of a stagnation layer of gas compressed between the spark channels. Spark channels initiated without equal amounts of preionization laser energy do not grow symmetrically and the stronger shock of the larger arc channel is able to penetrate into the weaker, smaller arc channel. The geometrical form of the individual channels is maintained long into the recovery phase of the spark ($>$ 1 ms) suggesting that the channels recover individually as opposed to mixing together. Lighter gas mixtures exhibit some turbulent mixing at the interface of the two channels.

The voltage drop and resistance of a dual channel spark gap are only slightly smaller than that of a spark gap operating through a single channel. This results from a lower heating rate and hence, smaller electrical conductivity, and a smaller rate of expansion of the individual columns in a dual channel spark gap as compared to a single channel. The reduced electron temperature in dual channel arcs is implied from the interferometric fringe shift data that shows a reduced inner-core electron density. A scaling model for the resistance of multichannel spark gaps for our conditions using Spitzer conductivity, arc expansion, and current sharing agrees well with experiment.

ACKNOWLEDGMENTS

The authors wish to thank Dr. E. A. Crawford at Spectral Technology, Inc. (STI), and Dr. R. J. Gripshover, Dr. E. D. Ball, and Dr. D. B. Fenneman at the Naval Surface Weapons Center for their helpful input during these measurements. The authors also wish to acknowledge D. M. Barrett of STI who designed the pulsed power system for the experiment. This work was supported by the Naval Surface Weapons Center, Contract No. N60921-83-C-4057.

[1]R. S. Taylor and K. E. Leopold, Rev. Sci. Instrum. **55**, 52 (1984).
[2]C. L. M. Ireland, J. Phys. E **8**, 1007 (1975).
[3]J. R. Woodworth, C. A. Frost, and T. A. Green, J. Appl. Phys. **53**, 4734 (1982).
[4]J. R. Woodworth, R. G. Adams, and C. A. Frost, IEEE Trans. Plasma Sci. **PS-10**, 257 (1982).
[5]J. R. Woodworth, P. J. Hargis, Jr., L. C. Pitchford, and R. A. Hamil, J. Appl. Phys. **56**, 1382 (1984).
[6]L. P. Bradley and T. J. Davies, IEEE J. Quantum Electron. **QE-7**, 464 (1971).
[7]A. H. Guenther and J. R. Bettis, J. Phys. D **11**, 1577 (1978).
[8]R. S. Taylor, A. J. Alcock, and K. I. Leopold, "Laser Triggered Rail Gaps," in *Conference Proceedings IEEE Fourteenth Pulse Power Modulator Symposium*, Orlando, FL (IEEE, New York, 1980), p. 32.
[9]W. D. Kimura, E. A. Crawford, M. J. Kushner, and S. R. Byron, "Investigation of Laser Preionization Triggered High Power Switches Using Interferometric Techniques," in *Conference Record of 1984 Sixteenth Power Modulator Symposium*, Arlington, VA (IEEE, New York, 1984), p. 54.
[10]D. M. Barrett, S. R. Byron, E. A. Crawford, D. H. Ford, and W. D. Kimura, *A Novel Low Inductance Capacitive High Voltage Probe for Spark Gap Measurements*, 1985 High Voltage Workshop, Monterey, CA (unpublished).
[11]D. M. Barrett, S. R. Byron, E. A. Crawford, D. H. Ford, W. D. Kimura, and M. J. Kushner, Rev. Sci. Instrum. (to be published).
[12]M. J. Kushner, W. D. Kimura, and S. R. Byron, J. Appl. Phys. **58**, 1744 (1985).
[13]M. J. Kushner, R. D. Milroy, and W. D. Kimura, J. Appl. Phys. **58**, 2988 (1985).
[14]H. C. Harjes, E. E. Kunhardt, M. Kristiansen, L. L. Hatfield, and H. H. Guenther, IEEE Trans. Plasma. Sci. **PS-10**, 261 (1982).
[15]M. Mitchner and C. H. Kruger, *Partially Ionized Gases* (Wiley-Interscience, New York, 1973), p. 99.
[16]J. C. Martin, AWRE Report No. SSWA/JCM/1065/25, 1965.